

- and W. van Haringen, *Phys. Status Solidi* **37**, 709 (1970).
- ⁴G. Feher, *Phys. Rev.* **114**, 1219 (1959).
- ⁵E. B. Hale and R. L. Mieher, *Phys. Rev.* **184**, 751 (1969).
- ⁶T. G. Castner, Jr., *Phys. Rev. B* **2**, 4911 (1970), and references therein.
- ⁷W. Kohn, in *Solid State Physics*, edited by F. Seitz and D. Turnbull (Academic, New York, 1957), Vol. 5, p. 257.
- ⁸G. E. G. Hardeman, *J. Phys. Chem. Solids* **24**, 1223 (1963).
- ⁹D. R. Hamilton, W. J. Choyke, and Lyle Patrick, *Phys. Rev.* **131**, 127 (1963).
- ¹⁰A. H. Gomes de Mesquita, *Acta Cryst.* **23**, 610 (1967).
- ¹¹H. H. Woodbury and G. W. Ludwig, *Phys. Rev.* **124**, 1083 (1961).
- ¹²A. Taylor and R. M. Jones, in *Silicon Carbide*, edited by J. R. O'Connor and J. Smiltens (Pergamon, New York, 1960), p. 147.
- ¹³W. J. Choyke, D. R. Hamilton, and Lyle Patrick, *Phys. Rev.* **133**, A1163 (1964).
- ¹⁴W. J. Choyke and Lyle Patrick, *Phys. Rev.* **127**, 1868 (1962).
- ¹⁵J. L. Birman, *Phys. Rev.* **115**, 1493 (1959); T. K. Bergstresser and M. L. Cohen, *ibid.* **164**, 1069 (1967).
- ¹⁶D. W. Feldman, J. H. Parker, Jr., W. J. Choyke, and Lyle Patrick, *Phys. Rev.* **170**, 698 (1968).
- ¹⁷H. Jones, in *The Theory of Brillouin Zones and Electronic States in Crystals* (North-Holland, Amsterdam, 1960), p. 148.
- ¹⁸Lyle Patrick, D. R. Hamilton, and W. J. Choyke, *Phys. Rev.* **143**, 526 (1966).
- ¹⁹A. R. Verma and P. Krishna, *Polymorphism and Polytypism in Crystals* (Wiley, New York, 1966).
- ²⁰The electron density on the favored sc sublattice sites is nine times that on the other C sites, omitting any adjustment for distance from the donor.
- ²¹P. J. Dean and Lyle Patrick, *Phys. Rev. B* **2**, 1888 (1970).
- ²²This effect would be easier to see in GaP, which also has a zinc-blende lattice with conduction-band minima at X. The C+S pair spectrum is a good one to study as a function of excitation intensity.
- ²³There is not a standard notation for representations, and what we call M_3 is sometimes called M_4 . We follow the notation of Refs. 2 and 3.
- ²⁴G. B. Wright and A. Mooradian, *Phys. Rev. Letters* **18**, 608 (1967).
- ²⁵There may be three different values of both $\eta(\text{Si})$ and $\eta(\text{C})$ in 6H SiC, but this additional complexity will not be considered.
- ²⁶Lyle Patrick and W. J. Choyke, *Phys. Rev. B* **2**, 2255 (1970).
- ²⁷Also, it is not yet certain that the luminescence spectrum of Ref. 9 is correctly attributed to exciton recombination at nitrogen ions.
- ²⁸D. R. Hamilton, Lyle Patrick, and W. J. Choyke, *Phys. Rev.* **138**, A1472 (1965).

Photoluminescence Associated with Multivalley Resonant States of the N Isoelectronic Trap in $\text{In}_{1-x}\text{Ga}_x\text{P}^\dagger$

D. R. Scifres, H. M. Macksey, N. Holonyak, Jr., R. D. Dupuis, and G. W. Zack
*Department of Electrical Engineering, Materials Research Laboratory,
 and Coordinated Science Laboratory, University of Illinois at Urbana-Champaign, Urbana, Illinois 61801*

and

C. B. Duke, G. G. Kleiman, and A. B. Kunz
*Department of Physics, Materials Research Laboratory, and Coordinated Science Laboratory,
 University of Illinois at Urbana-Champaign, Urbana, Illinois 61801*

(Received 7 October 1971)

Line emission above the direct interband threshold is observed at 77 °K in $\text{In}_{1-x}\text{Ga}_x\text{P:N}$ for $0.59 \leq x \leq 0.71$. This emission is identified with a resonance state of the N isoelectronic trap whose properties are evaluated by standard solid-state scattering theory. For $x \geq 0.71$ the nitrogen trap state lies below both the direct and indirect interband thresholds. In this case the sharp, fast, nitrogen A line can be distinguished clearly from the slower, broad N-N pair spectra.

I. INTRODUCTION

In a recent Letter¹ we reported photostimulated line emission above the direct interband threshold associated with a resonance state of the N isoelectronic trap in $\text{GaAs}_{1-x}\text{P}_x$. It was suggested that a firm confirmation of the interpretation of these earlier data¹ would be the observation of a similar

phenomenon in $\text{In}_{1-x}\text{Ga}_x\text{P:N}$ for $x \sim 0.7$. In this paper we report such an observation. In addition, the data and theory reported earlier for $\text{GaAs}_{1-x}\text{P}_x:\text{N}$ are extended in several directions for the system $\text{In}_{1-x}\text{Ga}_x\text{P:N}$, $0.5 < x \leq 1.0$. First, the photoluminescence spectra are compared with absorption spectra to identify the energy of the band edge in our samples. Because the N state is above

the Γ band edge for $x < 0.71$, it is worth noting that accidentally introduced concentrations of N in $\text{In}_{1-x}\text{Ga}_x\text{P}$ could cause the "apparent" band gap to move to higher energies if the concentration of the nitrogen were uncontrolled. This effect has not been recognized previously. Second, studies of the emission line shapes from $\text{In}_{1-x}\text{Ga}_x\text{P}:\text{N}$ in the composition range $x \geq 0.71$, for which the nitrogen trap lies below the conduction-band minima at both Γ and X , permits the distinction between sharp, fast, nitrogen A -line emission and broad, slower, N-N pair emission.² Finally, we present the details of our model calculations of the spectral density associated with the ground state of the nitrogen impurity in III-V mixed-crystal alloys. Although it is crude, the model seems adequate to describe the qualitative features of the data. Refinements of the model are complicated and probably unreliable.³

We proceed by presenting the experimental data on $\text{In}_{1-x}\text{Ga}_x\text{P}:\text{N}$ in Sec. II. In Sec. III the details of this model calculations are described, and numerical results for $\text{In}_{1-x}\text{Ga}_x\text{P}:\text{N}$ are presented. Finally, in Sec. IV, we note the major limitations on the experimental data, the model used in the calculations, and the comparison between the calculations and the data.

II. EXPERIMENTAL PROCEDURE AND RESULTS

A. Crystal Preparation

As we have described elsewhere,⁴⁻⁶ the crystals of this work are grown by a modified Bridgman solution-growth technique utilizing an In solvent and InP and GaP source crystal. The source InP and GaP are introduced into solution at somewhat higher temperature (10–20 °C) than the growth temperature of the desired $\text{In}_{1-x}\text{Ga}_x\text{P}$, which is deposited deliberately in a region of essentially constant temperature (925–1000 °C). To make it easier to establish a temperature difference within the In solution between source and deposited crystal and to keep the source material separated from the $\text{In}_{1-x}\text{Ga}_x\text{P}$ ternary-crystal product, we use an hour-glass-shaped synthesis ampoule charged with InP and GaP and any desired dopants, e. g., in the present case GaN or Te. $\text{In}_{1-x}\text{Ga}_x\text{P}$ is grown slowly (20–30 days) at the other end of the ampoule. The crystal composition x , which is determined by electron microprobe analysis, is increased by raising the synthesis temperature and by increasing the source GaP/InP ratio. The $\text{In}_{1-x}\text{Ga}_x\text{P}$ crystals synthesized in this manner exhibit excellent local homogeneity and are the only ones that have been of sufficient quality to exhibit stimulated emission, both optically pumped⁴⁻⁶ and via junction injection.⁷

As in our earlier work,⁴⁻⁶ the as-grown $\text{In}_{1-x}\text{Ga}_x\text{P}$ ingots are sliced into wafers, polished to a thickness of $\sim 25 \mu$, and etched to a final thickness of 1–5 μ . The etched samples are cleaved into 25–

100- μ slivers, placed on flattened In wetted onto a copper heat sink, and compressed with a sapphire or diamond window into the In. This method of crystal mounting, for optical pumping through the transparent window, is particularly useful because it improves the sample optical Q and provides an efficient heat sink.⁹

B. Emission and Absorption Results

In order to reduce ambiguity in the experimental results and increase the reliability in their interpretation, we make comparative measurements (77 °K) of photoluminescence (emission spectra) on 1–5- μ samples with transmission (absorption) on 100–300- μ samples. In performing the emission measurements the samples are excited with a Spectra-Physics model-165 argon-ion laser. The transmission measurements are made on a Cary 14-RI spectrophotometer. The results obtained are fundamentally quite different, depending upon whether the sample composition x is less than or greater than $x \approx 0.71$. As shown below, this is the crystal composition at which the nitrogen A line is degenerate with the Γ band edge.

It seems appropriate to note that much of our discussion in this paper of the system $\text{In}_{1-x}\text{Ga}_x\text{P}:\text{N}$ is analogous to that given in our previous studies^{1,10} of $\text{GaAs}_{1-x}\text{P}_x:\text{N}$. Our absorption data on direct and indirect $\text{In}_{1-x}\text{Ga}_x\text{P}:\text{N}$ are entirely analogous to similar data (unpublished) on $\text{GaAs}_{1-x}\text{P}_x:\text{N}$ doped only with N and exhibiting only N-N pair (smeared owing to alloy disorder) and A -line absorption. In addition, our absorption measurements on $\text{GaAs}_{1-x}\text{P}_x:\text{N}$ are in complete agreement with the photoluminescence and laser behavior¹⁰ of these samples.

The major qualitative feature of our measurements on both $\text{GaAs}_{1-x}\text{P}_x:\text{N}$ and $\text{In}_{1-x}\text{Ga}_x\text{P}:\text{N}$ is the predominance in both the absorption and photoluminescence spectra of phenomena associated with the nitrogen impurity. For example, we have yet to examine a sample of either $\text{GaAs}_{1-x}\text{P}_x:\text{N}$ or $\text{In}_{1-x}\text{Ga}_x\text{P}:\text{N}$ that exhibits a strong (narrow) A line and does not also give a strong lower-energy absorption and emission. In fact, when N is known to be in a ternary crystal, particularly at concentrations ($> 10^{17}/\text{cm}^3$) exceeding any donor or acceptor doping, the broad, lower-energy emission is dominant.¹⁰ Also, if the N doping approaches $10^{19}/\text{cm}^3$, it then becomes very difficult to excite the crystal sufficiently to see anything but this low-energy emission.¹⁰ Because of the universality of our observations of such low-energy structure associated with the presence of nitrogen, and our consistent verification that even at several hundred meV below the A line this structure is quite sensitive to the nitrogen concentration, we provisionally identify it with N-N pair spectra.² We cannot, of

course, eliminate completely the possibility that some of the low-energy structure is associated with donor-acceptor pair recombination. Although this reservation should be kept in mind during the ensuing discussion, we can find no evidence that donor-acceptor pairs play any major role in the phenomena observed in our samples.

Typical results are shown in Fig. 1 on a sample of composition $x=0.68$ where the crystal is direct ($x \leq 0.74$)^{6, 11-13} and the *A* line appears in the Γ continuum ($x < 0.71$). The *N* in this sample was introduced accidentally in the long crystal-growth cycle, probably from SiN contamination of the quartz ampoule.¹⁴ The transmission results in Fig. 1 show that absorption begins on N-N pairs (NN in Fig. 1) at wavelengths near 6100 Å (2.032 eV) and extends to wavelengths shorter than 5600 Å (2.214 eV). Near 5560 Å (2.230 eV) the Γ band-edge absorption, as shown, rapidly cuts off the transmission, and the *A* line (higher in energy than the Γ band edge) is not observed in transmission. However, as shown at the top of Fig. 1, the *A* line is seen in emission,¹ as well as all of the features seen at the bottom of Fig. 1 in transmission. The *A* line is narrow. As we have described elsewhere for GaAsP:N,¹⁰ it is expected to be a fast transition, which is most important for stimulated emission studies. In contrast to the *A* line, and unlike GaP:N,² the transitions involving N-N pairs are broad (cf. Figs. 1 and 2) because, as in GaAs_{1-x}P_x:N with its random As-P distribution,

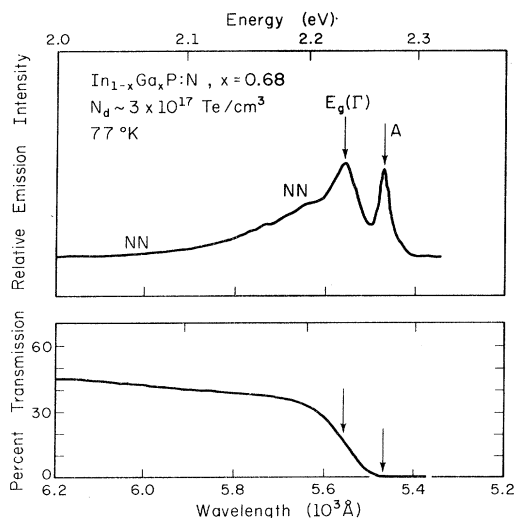


FIG. 1. Photoluminescence (10^2 -W/cm² sample excitation) and transmission (130- μ sample) spectra (77 °K) of direct In_{1-x}Ga_xP ($x=0.68$) doped with nitrogen. The direct-gap energy is labeled $E_g(\Gamma)$. The effect of nitrogen can be seen by lower-energy N-N pair recombination radiation and narrow *A*-line emission, above $E_g(\Gamma)$, which is not seen in transmission because of absorption on $E_g(\Gamma)$. The nitrogen concentration exceeds that of the Te.

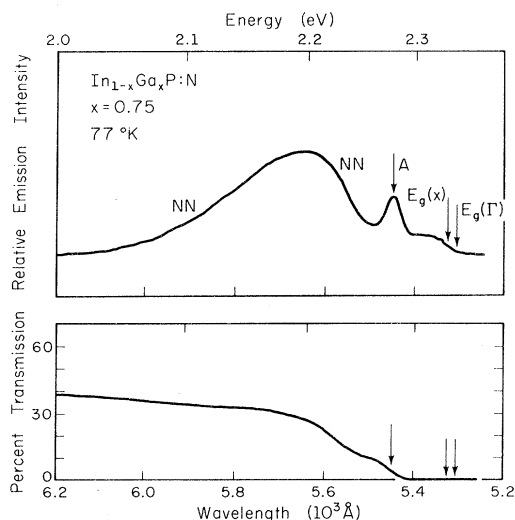


FIG. 2. Photoluminescence (10^4 -W/cm² sample excitation) and transmission (260- μ sample) spectra (77 °K) of indirect In_{1-x}Ga_xP ($x=0.75$) doped with nitrogen. The lower-energy emission and absorption are characteristic of nitrogen pair (NN) and *A*-line recombination below both the indirect $E_g(X)$ and direct $E_g(\Gamma)$ energy bands. *A*-line absorption cuts off transmission below $E_g(X)$ and $E_g(\Gamma)$. The only intentional dopant in this sample was nitrogen.

the distribution of In-Ga in In_{1-x}Ga_xP disturbs the potential in the region of N-N pairs.

The behavior of samples with $x > 0.71$ is illustrated by the data shown in Fig. 2 for a deliberately N-doped (and otherwise undoped) In_{1-x}Ga_xP crystal of composition $x \approx 0.75$. For $x > 0.71$ the nitrogen *A* line and the N-N pair transitions are lower in energy than both the Γ and *X* band minima. Consequently, as shown in Fig. 2, at wavelengths as long as 6000 Å (2.066 eV) N-N pair transitions begin to attenuate the transmission of the sample and, as indicated, at 5470 Å (2.267 eV) the *A* line cuts off the transmission so effectively that no band-edge absorption is evident. On the other hand, because of the rather high excitation levels achieved by the pumping technique described above, in emission we observe N-N pair, *A*-line, and weak band-to-band transitions. All of these are shown in Fig. 2. They are consistent with the transmission data. For a sample of composition $x \sim 0.75$, $E_g(\Gamma)$ and $E_g(X)$ are nearly equal and make it difficult to be precise in identifying the band-edge emission (cf. Fig. 2).

C. Position of Nitrogen *A* Line in In_{1-x}Ga_xP

From the above and related data obtained in our laboratory we have determined the position of the nitrogen *A* line in In_{1-x}Ga_xP in the composition range $0.59 \leq x \leq 1.0$. These results are shown in Fig. 3 on the Γ -*X* curve of Lorenz and Onton¹¹⁻¹³

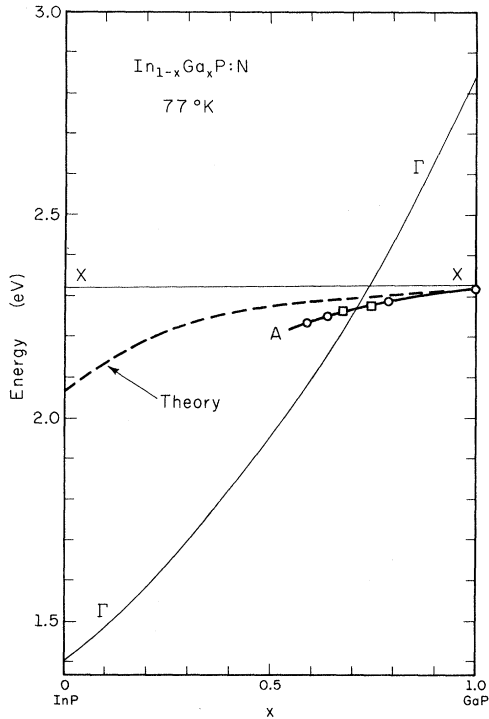


FIG. 3. Dependence of the nitrogen A-line energy on alloy composition in $\text{In}_{1-x}\text{Ga}_x\text{P}$ (77 °K) for the range $0.59 \leq x \leq 1.0$. The dashed curve indicates the dependence expected from a calculation using a constant electron-nitrogen central-cell potential (see Sec. III). The two square data points at $x=0.68$ and 0.75 correspond to the A-line data of Figs. 1 and 2, respectively. Solid lines are the Γ -X curves (adjusted to 77 °K) of Lorenz and Onton (Refs. 10–12). If the strength of the potential of the N isoelectronic trap is taken to increase linearly with $1-x$ so that the theoretical curve passes through the two square experimental points, then the trap state in InP occurs at $E_R \approx 1.97$ eV.

adjusted to 77 °K.⁶ Also shown is the behavior of the A line predicted by a simple model calculation¹ which will be discussed in detail in Sec. III. The two square data points of Fig. 3, i.e., the points at $x=0.68$ and 0.75 , correspond to the A-line data of Figs. 1 and 2, respectively. Not indicated in Fig. 3 with a data point is the fact that the $E_f(\Gamma)$ energy identified in Fig. 1 ($x=0.68$) agrees perfectly with the Γ curve of Lorenz and Onton.^{11–13} This point together with those taken from other data at $x=0, 0.27, 0.41,$ and 0.59 ⁶ agree with the entire Γ curve, including the position of the direct-indirect transition. That is, the results we present here, viz., the behavior of the nitrogen A line in $\text{In}_{1-x}\text{Ga}_x\text{P}$ with crossover into the Γ continuum at $x=0.71$, automatically implies that the direct-indirect transition occurs at $x>0.71$. Otherwise, the X band edge would have to lie in position below the A line, which is not the case experimentally,

or theoretically as will be discussed below (Sec. III).

III. MODEL CALCULATION

A. Description of Model

Isoelectronic impurities have been classified as either acceptors, if they attract electrons, or donors, if they attract holes.¹⁵ An isoelectronic acceptor, such as N in $\text{GaAs}_{1-x}\text{P}_x$ or $\text{In}_{1-x}\text{Ga}_x\text{P}$, presumably binds an exciton by first binding an electron in the conduction band via a short-range attractive potential and then binding a hole via the Coulomb potential of the N-plus-electron system.³ The exciton either recombines radiatively or ionizes, with a branching ratio depending on the temperature.¹⁶

We present here a description of a model calculation which is simple but capable of explaining the main features of the observed x dependence of the photoluminescence data in $\text{In}_{1-x}\text{Ga}_x\text{P}$. Using solid-state scattering theory,^{17,18} we show the existence of a resonant state of the N impurity above the conduction-band minimum for $x \lesssim 0.71$ in $\text{In}_{1-x}\text{Ga}_x\text{P}$. This state results from the combined effects of the short-range nature of the potential associated with an isoelectronic trap³ and the electronic band structure of $\text{In}_{1-x}\text{Ga}_x\text{P}$.^{19–21} Several authors^{22–28} have interpreted strong photoluminescence associated with N traps in high-P ($x > 0.3$) $\text{GaAs}_{1-x}\text{P}_x$ samples, where the Γ minimum is above the energy of the bound exciton. However, the intense above-band-gap radiation due to the N trap, which we reported for $\text{GaAs}_{1-x}\text{P}_x$ earlier¹ and for $\text{In}_{1-x}\text{Ga}_x\text{P}$ in the present paper, has not been observed previously.

Our explanation of this above-band-gap radiation depends explicitly upon the short-range character of the potential of the N isoelectronic trap as opposed to the long-range Coulomb potential associated with shallow donors.^{27–30} In this context, it seems appropriate to note the existence of two other^{31,32} recent studies of resonant impurity states. However, the calculations discussed in these articles are considerably more complicated than ours and, moreover, are not in a form directly applicable to the isoelectronic-acceptor problem.

In order to explore the consequences of the short-range nature of the attractive N impurity potential, we employ the Koster-Slater one-band, one-site approximation,¹⁷ which has been shown to provide a qualitatively correct description of this potential in GaP.³ In this model, the impurity potential extends over only one lattice site and, in addition, is diagonal in the band indices. Thus, the matrix element of V , the attractive isoelectronic potential, between electron Wannier states is given by¹⁷

$$\langle \vec{R}_s, n | V | \vec{R}_t, m \rangle = V_0 \delta_{st} \delta_{nc} \delta_{mc} . \quad (3.1)$$

The quantities \vec{R}_s and n are, respectively, the site and band indices of the Wannier states. Equation (3.1) describes coupling only to the lowest-energy conduction band, denoted by the index c . We neglect the short-range repulsive impurity-hole interaction,³ since the hole ultimately is bound by the long-range Coulomb attraction of the electron. The probability $|\psi_B(0)|^2$ that the electron is in the (central) cell containing the impurity is given in the Wannier representation by¹⁸

$$|\psi_B(0)|^2 = |1 - V_0\Lambda(E)|^{-2}, \quad (3.2a)$$

$$\Lambda(E) \equiv \lim_{\delta \rightarrow 0^+} \int_{-\infty}^{\infty} dt N(t)/(E - t + i\delta) \quad (3.2b)$$

In Eq. (3.2b), the quantity $N(t)$ is the density of states in the lowest-energy conduction band of the host material.

The expressions in Eqs. (3.2) reflect the short-range nature of the attractive N potential in that the one-electron eigenstates of the impurity potential are linear combinations of Bloch states associated with values of momentum throughout the first Brillouin zone.²⁷ If the ground state of the impurity exists, it exists as a single discrete localized state whose energy is a function of the composition x in $\text{In}_{1-x}\text{Ga}_x\text{P}$.

In order to calculate $|\psi_B(0)|^2$, we compute both the band structure and the electronic density of states via the empirical pseudopotential method.^{33,34} For pure $\text{In}_{1-x}\text{Ga}_x\text{P}$, we use the values

$$V_{\vec{K}}(\text{In}_{1-x}\text{Ga}_x\text{P}) = xV_{\vec{K}}(\text{GaP}) + (1-x)V_{\vec{K}}(\text{InP}) \quad (3.3)$$

for the pseudopotential form factors. The form factors for GaP and InP were obtained from Cohen and Bergstresser¹⁹ and the lattice constant a was obtained by scaling those¹⁹ for GaP and InP in the fashion noted in Eq. (3.3). The density of states was evaluated for each of the bands individually and for three regions of the Brillouin zone separately: $0 \leq k_i a/2\pi \leq 0.125$, $0.125 \leq k_i a/2\pi \leq 0.5$, and $0.5 \leq k_i a/2\pi$ up to the boundaries of the first Brillouin zone. The quantities k_i denote the components of the electronic wave vector \vec{k} and we refer to the three regions as regions Γ , II, and X , respectively. We parametrize the densities of states in a form³⁵ which yields an analytic expression for $\Lambda(E)$. A study of the alloy band structures¹ reveals that to within the accuracy of the model this parametrization depends upon x only via the energies of the conduction band at Γ , X , and L . Since there is some question about the adequacy of the empirical pseudopotential method,^{20,21} we use the E_X and E_{Γ} values of Lorenz and Onton¹¹⁻¹³ in our parametrization.

Although this model of the density of states is rather crude, its sophistication is comparable to that of the simple model of the attractive impurity potential given in Eq. (3.1). As it has been shown

to be qualitatively accurate in the case of resonant N-trap states in $\text{GaAs}_{1-x}\text{P}_x$,¹ it suffices for our present purposes.

B. Construction of Solvable Model

If we divide the first Brillouin zone into the regions described in Sec. IIIA, we can express the total density of states as a sum of the densities of states contributed by each of the different regions. Thus, we can write

$$N(E) = \sum_{\alpha} N_{\alpha}(E). \quad (3.4a)$$

The subscript α denotes the different regions of the zone. Let us parametrize N_{α} in Newns's³⁵ form,

$$N_{\alpha}(E) = C_{\alpha} \Delta_{\alpha} (1 - u_{\alpha}^2)^{1/2} \theta(1 - |u_{\alpha}|), \quad (3.4b)$$

$$u_{\alpha} \equiv (E - E_{\alpha} - \Delta_{\alpha})/\Delta_{\alpha}, \quad (3.4c)$$

$$\int_{-\infty}^{\infty} dE N_{\alpha}(E) = \frac{1}{2\pi} C_{\alpha} \Delta_{\alpha}^2. \quad (3.4d)$$

In Eq. (3.4b), $\theta(x)$ denotes the unit-step function. The parameter Δ_{α} is determined from the extent in energy of the density of states in the region labeled by α as determined from numerical computations with the empirical pseudopotential method for concentrations such that the minima at Γ and X are equal (i. e., $x \approx 0.5$ in $\text{GaAs}_{1-x}\text{P}_x$ and $x \approx 0.7$ in $\text{In}_{1-x}\text{Ga}_x\text{P}$). In addition, C_{α} is chosen so that $\frac{1}{2} C_{\alpha} \pi \Delta_{\alpha}^2$ is equal to the normalized integrated computed density of states in the region labeled by α . After this determination, C_{α} and Δ_{α} are taken to be independent of x . This procedure results in the values $C_X = 0.3675 \text{ eV}^{-2}$, $\Delta_X = 1.55 \text{ eV}$, $C_{\Gamma} = 0.0183 \text{ eV}^{-2}$, and $\Delta_{\Gamma} = 0.8 \text{ eV}$ for $\text{GaAs}_{0.5}\text{P}_{0.5}$. In this material, we can ignore the contributions to the density of states from region II, since the energy at L is never less than 1 eV above that at X . In $\text{In}_{1-x}\text{Ga}_x\text{P}$, on the other hand, we must include contributions from region II, since $E_{\Gamma} < E_L < E_X$ in InP .^{11-13,19-21} Fitting Eqs. (3.4) to the numerically computed densities of states for $\text{In}_{0.3}\text{Ga}_{0.7}\text{P}$ yields the values $C_X = 0.3034 \text{ eV}^{-2}$, $\Delta_X = 1.675 \text{ eV}$, $C_{\Gamma} = 0.0260 \text{ eV}^{-2}$, $\Delta_{\Gamma} = 0.625 \text{ eV}$, $C_{\text{II}} = 0.2346 \text{ eV}^{-2}$, and $\Delta_{\text{II}} = 1.325 \text{ eV}$. As in our calculations for $\text{GaAs}_{1-x}\text{P}_x$,¹ the energies of the minima at X and Γ are obtained from Lorenz and Onton.¹¹⁻¹³ The energy at L is determined by linearly extrapolating between the values given by Cohen and Bergstresser¹⁹ for InP and GaP.

By inserting Eqs. (3.4) into Eqs. (3.2), we obtain an analytic expression for $\Lambda(E)$,³⁵

$$\Lambda(E) = R(E) - i\pi N(E), \quad (3.5a)$$

$$R(E) \equiv \text{Re}\Lambda(E) = \sum_{\alpha} R_{\alpha}(E), \quad (3.5b)$$

$$R_{\alpha}(E) \equiv \pi C_{\alpha} \Delta_{\alpha} \{u_{\alpha} + (u_{\alpha}^2 - 1)^{1/2} [\theta(-u_{\alpha} - 1) - \theta(u_{\alpha} - 1)]\}. \quad (3.5c)$$

Using Eqs. (3.2), (3.4) and (3.5), we evaluate the bound-state and resonance energies and the corresponding spectral densities of N traps in semiconductor alloys such as $\text{GaAs}_{1-x}\text{P}_x$ and $\text{In}_{1-x}\text{Ga}_x\text{P}$. The one unspecified parameter, V_0 , which is given in Eq. (3.1), is fixed by the ground-state energy of the trap in GaP ^{3,16} (i. e., $E_B = 0.008$ eV). That is, we determine V_0 by the requirement that, for $x=1$,

$$V_0\Lambda(E_X - E_B) = 1. \quad (3.6)$$

C. General Features of Model Predictions: Two-Region Limit

In order to examine the general model predictions, we consider the case in which only the Γ and X regions are important (i. e., the case appropriate for $\text{GaAs}_{1-x}\text{P}_x$ ¹). We note that there is a concentration, x_c , at which the Γ and X minima cross, so that $E_X > E_\Gamma$ for $x_c < x \leq 1$ and $E_\Gamma > E_X$ for $0 \leq x < x_c$. Further, we assume that there is a bound impurity state for $x=1$ determined by Eq. (3.6).

It is convenient to distinguish two cases. In the first of these, we assume equal densities of states at Γ and X , so that $C_X = C_\Gamma = C$ and $\Delta_X = \Delta_\Gamma = \Delta$ in Eqs. (3.4). In the second case the density of states at Γ is much less than that at X . Thus, in this example, $\Delta_\Gamma \sim \Delta_X$ and $C_\Gamma \ll C_X$, as in $\text{GaAs}_{1-x}\text{P}_x$, where the density of states at X is approximately 30 times that at Γ .¹ The resonant or bound-state energy E_R is determined by the following condition¹⁶:

$$V_0R(E_R) = 1. \quad (3.7)$$

The concentration dependence of E_R resulting from Eq. (3.7) can be determined in the case of equal densities of states at Γ and X from Fig. 4(a). When $x=1$, E_Γ is at its highest position relative to E_X . The condition that there be a bound state below X at this concentration in general requires that $V_0R(E_X)$ be greater than unity, since $R(E \rightarrow -\infty)$ approaches zero monotonically. In this case (i. e., $|E_\Gamma - E_X| > \Delta$), two bound states will exist as $x \rightarrow 1$: one associated with X and one with Γ . As x decreases, E_Γ moves downward toward E_X until, at some value of x , the higher-energy bound state disappears. As x is decreased still further, the single remaining bound state moves to lower energies until, in the configuration of E_Γ and E_X shown in Fig. 4(a), it is associated with Γ instead of X . If we increase $|E_X - E_\Gamma|$ still further relative to Δ , a (second) higher-energy resonant state associated with E_X appears which ultimately becomes a bound state when $|E_X - E_\Gamma| > 2\Delta$ (i. e., $x \rightarrow 0$).

We show in Fig. 4(a) the case when $V_0R_X(E_X) = V_0R_\Gamma(E_\Gamma) > 1$. In the situation that $V_0R_X(E_X) = V_0R_\Gamma(E_\Gamma) < 1$, a resonant or bound state exists

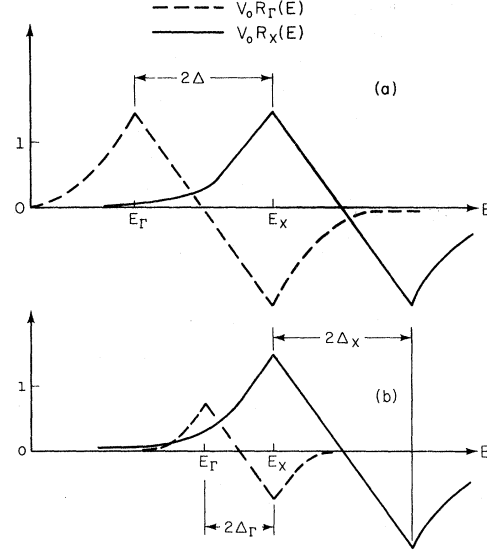


FIG. 4. Schematic illustration of the effect of the relative energies of the X and Γ minima upon the bound-state energy E_R according to the two-region model of Eqs. (3.4) and (3.5) and the bound-state conditions in Eqs. (3.6) and (3.7) (i. e., the bound-state energy is below E_X when $x=1$). In (a), we illustrate the case of equal densities of states at X and Γ . When $E_X < E_\Gamma$, $E_R < E_X$, and when $E_\Gamma < E_X$, $E_R < E_\Gamma$. The case that $V_0R_X(E_X) = V_0R_\Gamma(E_\Gamma) > 1$ is illustrated. In (b), we illustrate the case that the density of states at X is much greater than that at Γ (i. e., the case appropriate to $\text{GaAs}_{1-x}\text{P}_x$). For all relative positions of X and Γ , E_R is dominated by the position of X . When $E_\Gamma > E_X$, the localized impurity state is bound (i. e., $E_R < E_X < E_\Gamma$), but when $E_\Gamma < E_X$, the state is resonant (i. e., $E_\Gamma < E_R < E_X$). It is observable because of the small density of states at Γ .

only when E_Γ and E_X are sufficiently close to each other, i. e., $|E_X - E_\Gamma| \ll \Delta$ or $x \approx x_c$. The dependence of E_R on x can be determined from the appropriate figures analogous to Fig. 4(a). Our main point is elementary: The detailed results are easily determined and depend sensitively on the values of the parameters V_0 , E_Γ , and E_X .

In Fig. 4(b), we illustrate the situation of highly asymmetric bands (i. e., the density of state at X is much larger than that at Γ). In this case, $R_\Gamma(E_\Gamma) \ll R_X(E_X)$. Thus, the condition that there be a bound state for $x=1$ [i. e., Eqs. (3.6) and (3.7)] requires that $V_0R_X(E_X) > 1$. Using the values of the parameters C_α and Δ_α given in the description of the parametrization of the $\text{GaAs}_{1-x}\text{P}_x$ densities of states following Eqs. (3.4), and $V_0 = -0.611$ determined for this material from Eq. (3.6), we find $V_0R_X(E_X) = 1.09$.

From these considerations and Fig. 4(b), we see that the bound state or resonant energy is determined largely by the value of E_X . For $x > x_c$ (i. e., $E_\Gamma > E_X$), Eq. (3.7) is satisfied for $E_R < E_X$, so that

bound states occur. As x approaches x_c the rising portion of $V_0 R_\Gamma(E_\Gamma)$ (i. e., for $E < E_\Gamma$) moves toward lower energies, so that $E_X - E_R$ increases. After the minima cross (i. e., $x < x_c$), a resonant state of energy $E_\Gamma < E_R < E_X$ appears. As the concentration x decreases further, $R_\Gamma(E)$ moves toward lower energies, and the effect of the Γ minimum upon the resonant-energy position diminishes so that $|E_X - E_R|$ decreases with x . However, there always remains some effect of the states at Γ on the value of E_R .

The interpretation of these results is simple. The condition that there be a bound state in the gap for $x=1$ requires that V_0 be of sufficient magnitude to satisfy Eq. (3.6). As the concentration decreases and the Γ minimum moves below the X minimum, localized states appear as either bound states in the gap or resonant states in the continuum (i. e., $E_X > E_R > E_\Gamma$). A high density of states at Γ pulls a bound state into the gap, since overlap with the continuum in this case prevents the existence of bound states in the allowed band.²⁷ A much lower density of states at Γ than at X causes the existence of resonant states in the continuum at Γ . The energy of these states is determined largely by the high density of states at X , although the influence of the Γ minimum lowers the resonant energy relative to the bound-state energy in pure GaP. The width of these states in energy is determined by the low density of states at Γ .¹

These predictions and their interpretation are in agreement with the findings of Bir,³¹ who treats shallow impurity states lying in an allowed band with the effective-mass method. He concludes that the states at Γ always increase the binding energy of the local state associated with a subsidiary minimum. This result, of course, neglects the consequences of the negative portions of the functions $V_0 R(E)$ shown in Fig. 4.

D. Results for $\text{In}_{1-x}\text{Ga}_x\text{P:N}$

In order to apply the model described in Secs. IIIA–IIIC to the mixed-crystal system $\text{In}_{1-x}\text{Ga}_x\text{P:N}$, it is necessary to account for the fact that the conduction-band energy at L moves below that of X for $x \lesssim 0.3$. For InP ,¹⁹ $E_L = 2.0$ eV, while for GaP , $E_L = 2.7$ eV. The Γ and X energies in InP ^{11–13} are $E_\Gamma = 1.35$ eV and $E_X = 2.25$ eV, while the corresponding energies in GaP ^{11–13} are $E_\Gamma = 2.78$ eV and $E_X = 2.26$ eV. We determine E_L as a function of x by linearly interpolating between the above two points. This x dependence of E_L requires use of a three-region model. The values of the parameters C_α and Δ_α resulting from parametrizing the numerically computed densities of states for $\text{In}_{0.3}\text{Ga}_{0.7}\text{P}$ according to Eqs. (3.4) are $C_X = 0.3034$ eV⁻², $\Delta_X = 1.675$ eV, $C_\Gamma = 0.260$ eV⁻², $\Delta_\Gamma = 0.625$ eV, $C_{II} = 0.2346$ eV⁻², and $\Delta_{II} = 1.325$ eV.

In Fig. 5, we show the resulting values for $|\psi_E(0)|^2$ as a function of E for various alloy concentrations. For $x > 0.71$, a single localized state exists below both the energy-band minima at Γ and X . For $x < 0.71$ this state becomes a resonance overlapping the continuum states near Γ and broadened by them. The shift in E_R from its value in GaP is indicated in the theoretical curve in Fig. 3. The concentration dependence of E_R is dominated by the downward motion of the high-density-of-states region of the band structure associated with L , as discussed in Sec. IIIC. The width of the levels, γ , which is shown in the inset in Fig. 5, is determined by the overlap of the level with the continuum at Γ . The crosshatched area in the inset in Fig. 5 indicates the region of x for which $|\psi_E(0)|^2$ is highly asymmetric so that a width cannot be defined. The asymmetry occurs because, in this region of x , $E_R - E_\Gamma > \Delta_\Gamma$, and our parametrized form of N_Γ in Eq. (3.4b) becomes unrealistic. Since when $E_L < E_X$ the binding energy is determined largely by the position of L and not by Γ , we conclude that the theoretical values of E_R shown in Fig. 3 are a valid indication of the concentration dependence of the bound-state energy in this material.

The widths shown in the inset in Fig. 5 correspond to resonant-state lifetimes $\tau_e \sim 10^{-13}$ sec. These times are comparable to free-exciton trapping times in GaP³⁶ but are shorter than radiative-recombination lifetimes ($\tau_r \sim 10^{-8}$ sec) for excitons

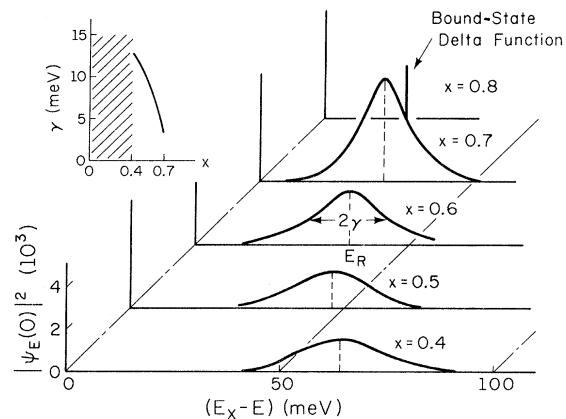


FIG. 5. Electronic density of states in the central cell of a N atom substituted on the group-V sublattice of $\text{In}_{1-x}\text{Ga}_x\text{P}$. The calculation was performed following Eqs. (3.4) and (3.5) in the text using $\Delta_\Gamma = 0.625$ eV, $\Delta_X = 1.675$ eV, $\Delta_{II} = 1.325$ eV, $C_\Gamma = 0.026$ eV⁻², $C_X = 0.303$ eV⁻², and $C_{II} = 0.235$ eV⁻² obtained from numerical calculations of the density of states for $\text{In}_{0.3}\text{Ga}_{0.7}\text{P}$. The value of V_0 was adjusted to give $E_X - E_R = 8$ meV in GaP. It was taken not to vary as a function of alloy concentration x . The shaded area in the inset indicates a region of values of x for which the energy half-width γ of the resonant state is not well defined for the reasons described in the text.

bound to N traps in GaP.¹⁶ Therefore, we visualize the N impurity either as initially trapping an electron and subsequently a hole on time scales comparable to that of the autoionization of the electron level ($\tau_e \sim 10^{-13}$ sec) or as trapping a free exciton on such a time scale. The resulting exciton recombines radiatively on a longer time scale, $\tau_r \sim 10^{-8}$ sec. Evidently,¹ both the short-range attractive electronic potential of the N trap and the much lower density of states at X than at either X or L are significant aspects of our ability to observe luminescence from the resulting resonant state in $\text{In}_{1-x}\text{Ga}_x\text{P}$.

In Sec. III C, we demonstrated that the resonant state cannot lie in the continuum at X , because of the high density of states at X . Thus, the experimental positions of the nitrogen A line in Fig. 3 indicate that the direct-indirect transition occurs for some concentration $x > 0.71$, in support of the findings of Lorenz and Onton.¹¹⁻¹³

Several authors^{3, 15, 22-26, 37} have studied the effects of isoelectronic substitutions upon the optical properties in wide-band-gap semiconductors. Faulkner³ has estimated the oscillator strength of the A line in optical absorption. It is, therefore, appropriate to outline briefly the contributions of the localized isoelectronic impurity states that we have discussed to the optical absorption. From the assumption that the short-range attractive isoelectronic impurity potential confines the bound electron primarily to the (central) cell containing the impurity, the bound-state electronic wave function ψ_e can be written approximately in the form^{18, 38}

$$\psi_e(\vec{r}) \approx \psi_E(0)A_c(\vec{r}). \quad (3.8)$$

In Eq. (3.8), \vec{r} is the electronic position and A_c is the Wannier state of the lowest conduction band in the central cell. Therefore, the oscillator strength for optical absorption by the bound exciton, f , is approximately proportional to $|\psi_E(0)|^2$. From this proportionality and the form of $|\psi_E(0)|^2$ for bound or resonant states illustrated in Fig. 5, we can account for the A -line structure evident in optical-density measurements,³ since the absorption coefficient is proportional to the oscillator strength.³⁹

The model we have described in this section accounts for our observations (shown in Figs. 1-3) of the A line in $\text{In}_{1-x}\text{Ga}_x\text{P}$ and $\text{GaAs}_{1-x}\text{P}_x$.¹ The NN pair structure, however, appearing in our emission and transmission measurements (Figs. 1 and 2) cannot be explained so easily. Its interpretation awaits further analysis, which in turn requires the construction of accurate NN pair potentials, a quite difficult task.

IV. COMPARISON OF EXPERIMENT AND THEORY

We have performed photoluminescence and transmission measurements (see, e.g., Figs. 1 and 2)

on $\text{In}_{1-x}\text{Ga}_x\text{P}:\text{N}$ for a wide range of alloy compositions (i.e., $0.59 \leq x \leq 1.0$). The resulting values of the nitrogen A line are plotted in Fig. 3. Several features of the data are new. First, the x dependence of the A line indicates that, although the N state is in the band gap for $x \geq 0.71$, it appears above the Γ band edge for $x \leq 0.71$. Second, because of the high excitations achieved by our optical pumping technique,^{4-6, 9, 10} we are able to distinguish between sharp, fast, A -line emission and broad, slower, NN pair emission.^{2, 10}

We are able to interpret the x dependence of the A line as being a consequence of both the short-range attractive nature of the isoelectronic N-trap potential and the details of the band structure in $\text{In}_{1-x}\text{Ga}_x\text{P}$. In our model, the A -line emission is associated with a single bound ($x > 0.71$) or resonant ($x < 0.71$) electronic state of the isoelectronic N trap.¹ The trapped electron recombines with a hole bound by the (attractive) electronic Coulomb potential. The x dependence of the theoretically computed bound-state energy is indicated in Fig. 3. According to the general predictions of the theory described in Sec. III C, the position of the bound state is dominated by the x dependence of the band-structure energies E_X and E_L , since regions of the Brillouin zone containing X and L exhibit high densities of states. The width of the resonant state for $x \leq 0.71$ is determined by the (low) density of states at Γ . The computed widths are indicated in the inset in Fig. 5. These widths correspond to resonant-state lifetimes $\tau_e \sim 10^{-13}$ sec, which are of the order of magnitude of free-exciton trapping times in pure GaP³⁶ and are much shorter than radiative-recombination lifetimes ($\tau_r \sim 10^{-8}$ sec) for excitons bound to N traps in GaP.¹⁶ Thus, the isoelectronic N impurity is thought to trap the exciton either by first trapping an electron and then a hole on time scales comparable to that of the autoionization of the electron level ($\tau_e \sim 10^{-13}$ sec) or by trapping a free exciton on the same time scale. The resulting exciton recombines radiatively on a longer time scale, $\tau_r \sim 10^{-8}$ sec.

The predictions of the theory and the experimental observations provide a verification of the band structures proposed by Lorenz and Onton.¹¹⁻¹³ Our emission and transmission spectra agree with their Γ curve for $x < 0.71$. For higher x , the position of the A line and the theoretical requirement that the bound state be below the high-density-of-states continuum at X indicate that the direct-indirect transition occurs no lower than $x = 0.71$.

The major limitation on the experimental methods that we have used lies in the fact that the N concentration is not amenable to determination by electron microprobe or similar technique. At the present time the resulting indeterminacy hampers us in performing an exhaustive study of the effects of N

impurities upon the emission and transmission spectra.

There are more limitations upon the validity of the theoretical model. First, it is crude and, in its present form, does not permit analysis of any structure in the emission and absorption spectra other than the A line. For example, analysis of the NN pair spectra awaits a model which includes NN pair potentials. The second major limitation of the model is related to the parametrized form³⁵ of the density of states in Eq. (3.4). Since $E_L - E_\Gamma > \Delta_\Gamma$ for $x \lesssim 0.4$, the details of the parametrizations become important in determining $|\psi_E(0)|^2$ for these concentrations. In particular, $|\psi_E(0)|^2$ is an asymmetric function of energy for small values of x so that it becomes meaningless to define a width. This is illustrated in the crosshatched region in the inset in Fig. 5. The bound-state energy, however, is dominated by the downward motion of L , relative to X , as determined by linearly extrapolating between the values of E_L for InP and GaP given by Cohen and Bergstresser.¹⁹ We expect, therefore, that the x dependence of the theoretical bound-state

energy plotted in Fig. 5 is qualitatively accurate.

For all its limitations, the model is simple and able to provide qualitative interpretation of the experimental A-line observations solely on the basis of the short-range nature of the N trap and the details of the band structure in $\text{In}_{1-x}\text{Ga}_x\text{P}$. Indeed, our main result is the explicit demonstration, both experimentally and theoretically, of the enormous impact on the luminescent properties of a short-range trap potential, even when it is relatively weak. As this same feature of the potential proves crucial in achieving laser operation in GaP,⁴⁰ it seems that the role of isoelectronic traps like N in achieving efficient luminescent and laser devices may be substantially greater than previously recognized.

ACKNOWLEDGMENTS

We are indebted to K. A. Kuehl, B. L. Marshall, Y. A. Moroz, and V. Swanson for technical assistance and to the typing pool in the Materials Research Laboratory for their preparation of several drafts of the manuscript.

[†]Work supported in part by the Advanced Research Projects Agency under Contract No. HC 15-67-C-0221, by the National Science Foundation under Grant No. GK-18960, and by the Joint Services Electronics Program under Contract No. DAAB-07-67-C-0199.

¹D. R. Scifres, N. Holonyak, Jr., C. B. Duke, G. G. Kleiman, A. B. Kunz, M. G. Craford, W. O. Groves, and A. H. Herzog, *Phys. Rev. Letters* **27**, 191 (1971).

²D. G. Thomas and J. J. Hopfield, *Phys. Rev.* **150**, 680 (1966).

³R. A. Faulkner, *Phys. Rev.* **175**, 991 (1968).

⁴R. D. Burnham, N. Holonyak, Jr., D. L. Keune, D. R. Scifres, and P. D. Dapkus, *Appl. Phys. Letters* **17**, 430 (1970).

⁵R. D. Burnham, N. Holonyak, Jr., D. L. Keune, and D. R. Scifres, *Appl. Phys. Letters* **18**, 160 (1971).

⁶D. R. Scifres, H. M. Macksey, N. Holonyak, Jr., and R. D. Dupuis (unpublished).

⁷H. M. Macksey, N. Holonyak, Jr., D. R. Scifres, R. D. Dupuis, and G. W. Zack (unpublished).

⁸H. W. Korb, A. M. Andrews, N. Holonyak, Jr., R. D. Burnham, C. B. Duke, and G. G. Kleiman (unpublished).

⁹N. Holonyak, Jr. and D. R. Scifres (unpublished).

¹⁰N. Holonyak, Jr., D. R. Scifres, R. D. Burnham, M. G. Craford, W. O. Groves, and A. H. Herzog, *Appl. Phys. Letters* **19**, 254 (1971); N. Holonyak, Jr., D. R. Scifres, M. G. Craford, W. O. Groves, and D. L. Keune, *Appl. Phys. Letters* **19**, 256 (1971).

¹¹M. R. Lorenz and A. Onton, in *Proceedings of the Tenth International Conference on the Physics of Semiconductors, Boston, 1970* (U. S. Atomic Energy Commission, Oak Ridge, Tenn., 1970), pp. 444-449; A. Onton and M. R. Lorenz, in *Proceedings of the 1970 Symposium on GaAs and Related Compounds, Aachen, Germany* (Institute of Physics and the Physical Society, London, 1970), pp. 222-230.

¹²A. Onton and R. J. Chicotka, *Phys. Rev. B* **4**, 1847

(1971).

¹³A. Onton, M. R. Lorenz, and W. Reuter, *J. Appl. Phys.* **42**, 3420 (1971).

¹⁴E. D. Pierron, Monsanto Co., St. Louis (private communication).

¹⁵J. J. Hopfield, D. G. Thomas, and R. T. Lynch, *Phys. Rev. Letters* **17**, 312 (1966).

¹⁶J. D. Cuthbert and D. G. Thomas, *Phys. Rev.* **154**, 763 (1967).

¹⁷G. F. Koster and J. C. Slater, *Phys. Rev.* **95**, 1167 (1954).

¹⁸J. Callaway, *J. Math. Phys.* **5**, 783 (1964).

¹⁹M. L. Cohen and T. K. Bergstresser, *Phys. Rev.* **141**, 789 (1966).

²⁰J. A. Van Vechten and T. K. Bergstresser, *Phys. Rev. B* **1**, 3351 (1970).

²¹J. F. Hunter, G. Ball, and P. J. Morgan, *Phys. Status Solidi* **45**, 679 (1971).

²²D. G. Thomas, J. J. Hopfield, and C. J. Frosch, *Phys. Rev. Letters* **15**, 857 (1965).

²³D. G. Thomas and J. J. Hopfield, *Phys. Rev.* **150**, 680 (1966).

²⁴J. J. Hopfield, P. J. Dean, and D. G. Thomas, *Phys. Rev.* **158**, 748 (1967).

²⁵P. J. Dean and R. A. Faulkner, *Appl. Phys. Letters* **14**, 210 (1969).

²⁶P. J. Dean, *J. Luminescence* **1/2**, 398 (1970).

²⁷H. Kaplan, *J. Phys. Chem. Solids* **24**, 1593 (1964).

²⁸B. B. Kosicki and W. Paul, *Phys. Rev. Letters* **17**, 246 (1966); B. B. Kosicki, W. Paul, A. J. Strauss, and G. M. Iseler, *ibid.* **17**, 1175 (1966).

²⁹N. Holonyak, Jr., C. J. Nuese, M. D. Sirkis, and G. E. Stillman, *Appl. Phys. Letters* **8**, 83 (1966); M. G. Craford, G. E. Stillman, J. A. Rossi, and N. Holonyak, Jr., *Phys. Rev.* **168**, 867 (1968).

³⁰W. Paul, in *Proceedings of the Ninth International Conference on the Physics of Semiconductors, Moscow, 1968* (Nauka, Leningrad, 1968), Vol. I, p. 16.

³¹G. L. Bir, Fiz. Tverd. Tela **13**, 460 (1971) [Sov. Phys. Solid State **13**, 371 (1971)].

³²J. Callaway, Phys. Rev. B **3**, 2556 (1971).

³³D. Brust, J. C. Phillips, and F. Bassani, Phys. Rev. Letters **9**, 94 (1962).

³⁴D. Brust, M. L. Cohen, and J. C. Phillips, Phys. Rev. Letters **9**, 389 (1962).

³⁵D. M. Newns, Phys. Rev. **178**, 1123 (1969).

³⁶P. J. Dean, Phys. Rev. **168**, 889 (1968).

³⁷P. J. Dean, R. A. Faulkner, and S. Kimura, Phys. Rev. B **2**, 4062 (1971).

³⁸R. S. Knox, *Theory of Excitons* (Academic, New York, 1963).

³⁹F. Seitz, *The Modern Theory of Solids* (McGraw-Hill, New York, 1940).

⁴⁰N. Holonyak, Jr., D. R. Scifres, H. M. Macksey, R. D. Dupuis, Y. S. Moroz, C. B. Duke, G. G. Kleiman, and F. W. Williams, Phys. Rev. Letters **28**, 230 (1971).

Lattice Thermal Conductivity of p -Type GaSb in the Temperature Range 2–20 °K

K. S. Dubey and G. S. Verma

Physics Department, Banaras Hindu University, Varanasi-5, India

(Received 18 August 1971)

In the present paper the resonance-scattering relaxation rate for the electron-phonon interaction as given by Kumar *et al.* is used in the calculation of the resonance scattering of phonons by bound holes in p -type GaSb in the temperature range 2–20 °K. The present calculations show that with the simplified expressions of Kumar *et al.* for resonance scattering of phonons by bound electrons for $\omega > \omega_r$ and $\omega < \omega_r$, one can explain the anomalous resonance dip in the phonon-conductivity-vs-temperature curves of p -doped GaSb. An excellent agreement between theoretical and experimental values of phonon conductivity is obtained for the entire temperature range 2–20 °K on the basis of Callaway's model of phonon conductivity, provided one incorporates separate conductivity integrals for $0 < \omega < \omega_r$ and $\omega_r < \omega < \omega_D$, where ω_r is the resonance frequency and ω_D is the Debye frequency.

I. INTRODUCTION

Holland¹ measured the phonon conductivity of p -type GaSb in the temperature range 2–20 °K. He observed resonance dips in the phonon-conductivity-vs-temperature curves occurring at 5 °K. He considered the resonance scattering of phonons by the holes on the basis of Carruther's² theory but failed to explain his experimental results. Resonance dips in κ -vs- T curves are quite common for doped alkali halides, and they occur both below (in the boundary scattering region) and above the phonon conductivity maximum (phonon-phonon scattering region). However, there are few doped semiconductors for which the resonance dips can be detected, and they usually lie in the boundary scattering region. In Sb-doped Ge the resonance dip occurs at about 0.7 °K. In p -type GaSb Holland observed a very pronounced resonance dip at 5 °K. The slopes of κ -vs- T curves were found to be quite different from each other, both below and above the resonance region. In view of these anomalous features, the experimental results could not be explained consistently. A family of curves were plotted by Holland varying $\delta = r_0^2 \times (k_B/\hbar)^2/4v_s^2$ and $\gamma = G(k_B/4\Delta)^4$, where r_0 is the acceptor-hole radius, k_B is Boltzmann's constant v is average phonon velocity, 4Δ is the energy difference between the acceptor-hole ground state

and the next-higher energy state, and G is a constant proportional to the number of scattering centers. With the help of such curves he tried to reach some conclusions regarding different resonance-scattering parameters. It was obvious from these curves that no single curve could explain the experimental results in the entire temperature range.

Recently, Kwok,³ while discussing acoustic-phonon attenuation in doped Ge, considered both elastic and inelastic scatterings of phonons by bound donor electrons both from the donor-electron ground state and the next-higher energy state. He used perturbation theory as well as the Green's function approach for frequencies close to the resonance region. Kumar *et al.*⁴ obtained the simplified expressions from Kwok's theory both for $\hbar\omega_{q\lambda} \gg 4\Delta$ and $k_B T \gg 4\Delta$, and $\hbar\omega_{q\lambda} \ll 4\Delta$ and $k_B T \ll 4\Delta$, where 4Δ is the energy difference between the ground state and the next-higher energy state. These regions correspond to $\omega < \omega_r$ and $\omega > \omega_r$, is the resonance frequency. The resonance-scattering relaxation rate shows different frequency dependences in the different frequency regions. For $\omega < \omega_r$, $\tau_{ep}^{-1} \propto \omega^4$ for scattering off the ground state and $\tau_{ep}^{-1} \propto \omega^2$ for scattering off the next-higher energy state. For inelastic processes τ_{ep}^{-1} is independent of frequency. However, for $\omega > \omega_r$, $\tau_{ep}^{-1} \propto \omega^2$ both for elastic scattering and inelastic scattering processes. It